Organic & Biomolecular Chemistry

PAPER

View Article Online
View Journal | View Issue

Cite this: *Org. Biomol. Chem.*, 2015, **13**, 7928

A potent and selective C-11 labeled PET tracer for imaging sphingosine-1-phosphate receptor 2 in the CNS demonstrates sexually dimorphic expression†

Xuyi Yue,[a] Hongjun Jin,[a] Hui Liu,[a] Adam J. Rosenberg,[a] Robyn S. Klein*[b] and Zhude Tu*[a]

Sphingosine-1-phosphate receptor 2 (S1PR2) plays an essential role in regulating blood–brain barrier (BBB) function during demyelinating central nervous system (CNS) disease. Increased expression of S1PR2 occurs in disease-susceptible CNS regions of female *versus* male SJL mice and in female multiple sclerosis (MS) patients. Here we reported a novel sensitive and noninvasive method to quantitatively assess S1PR2 expression using a C-11 labeled positron emission tomography (PET) radioligand [^{11}C]**5a** for *in vivo* imaging of S1PR2. Compound **5a** exhibited promising binding potency with IC_{50} value of 9.52 ± 0.70 nM for S1PR2 and high selectivity over S1PR1 and S1PR3 (both IC_{50} > 1000 nM). [^{11}C]**5a** was synthesized in ~40 min with radiochemistry yield of 20 ± 5% (decayed to the end of bombardment (EOB), n > 10), specific activity of 222–370 GBq μmol^{-1} (decayed to EOB). The biodistribution study in female SJL mice showed the cerebellar uptake of radioactivity at 30 min of post-injection of [^{11}C]**5a** was increased by Cyclosporin A (CsA) pretreatment (from 0.84 ± 0.04 ID% per g to 2.21 ± 0.21 ID% per g, n = 4, p < 0.01). MicroPET data revealed that naive female SJL mice exhibited higher cerebellar uptake compared with males following CsA pretreatment (standardized uptake values (SUV) 0.58 ± 0.16 *vs.* 0.48 ± 0.12 at 30 min of post-injection, n = 4, p < 0.05), which was consistent with the autoradiographic results. This data suggested that [^{11}C]**5a** had the capability in assessing the sexual dimorphism of S1PR2 expression in the cerebellum of the SJL mice. The development of radioligands for S1PR2 to identify a clinical suitable S1PR2 PET radiotracer, may greatly contribute to investigating sex differences in S1PR2 expression that contribute to MS subtype and disease progression and it will be very useful for detecting MS in early state and differentiating MS with other patients with neuroinflammatory diseases, and monitoring the efficacy of treating diseases using S1PR2 antagonism.

Received 12th May 2015,
Accepted 9th June 2015

DOI: 10.1039/c5ob00951k

www.rsc.org/obc

1. Introduction

Multiple sclerosis (MS) is a neuroinflammatory demyelinating disease of the central nervous system (CNS) which leads to focal plaques of primary demyelination in conjunction with BBB disruption in the gray and white matter of the brain and spinal cord.[1,2] MS affects 2.5 million people worldwide with a prevalence of approximately 0.1% in the Caucasian population.[3] The life expectancy of patients with MS is significantly reduced and the quality of life is adversely affected in terms of mobility and social functioning. MS also has a strong sex bias, with the female to male ratio currently approaching 4 : 1.[4–6] Relapsing-remitting MS (RRMS), the most common form of the disease in women, is a condition in which recurrent episodes of new neurological dysfunction (relapses) are separated by periods of clinical stability (remission). Most RRMS patients (>50%) will develop secondary progressive MS (SPMS), with increased and sustained disability within 10–20 years after diagnosis.[7,8] The mechanisms of that contribute to progression of MS are incompletely understood.

Sphingolipids, main components of nervous tissue, have been linked to MS several decades ago. Nowadays, especially sphingosine-1-phosphate (S1P) is in the focus of pathophysiological research and therapy development. S1P is a membrane-derived lysophospholipid that binds with five subtype

[a]*Department of Radiology, Washington University School of Medicine, St. Louis, MO 63110, USA. E-mail: tuz@mir.wustl.edu; Fax: +1-314-362-8555; Tel: +1-314-362-8487*
[b]*Departments of Medicine, Anatomy & Neurobiology, Pathology & Immunology, Washington University School of Medicine, St. Louis, MO 63131, USA. E-mail: rklein@dom.wustl.edu; Fax: +1-314-362-9320; Tel: +1-314-286-2140*
†Electronic supplementary information (ESI) available. See DOI: 10.1039/c5ob00951k

G-protein coupled receptors S1PR1–S1PR5. The activation of S1PRs modulates a spectrum of key biological events including activities in the CNS and immune response.[9] Sphingolipid-like immunomodulator fingolimod (FTY-720, Gilenya) is the first oral disease-modifying therapy approved by the US Food and Drug Administration (FDA) for RRMS.[10] Phosphorylated Fingolimod sequesters lymphocytes within the lymph nodes and prevents their trafficking to the CNS, *via* binding to S1PR subtypes S1PR1, S1PR3, S1PR4, and S1PR5, but not S1PR2.[11] Encouraged by the success of Fingolimod, much effort has been devoted to developing selective compounds targeting S1PR subtypes, especially S1PR1 or S1PR2.[12]

In a recent study, we found increased expression of S1PR2 in disease-susceptible CNS regions of female MS patients, and suggest cell intrinsic sex differences in the S1PR2 expression on CNS vasculature contribute to the development of disease cycles in females compared with males.[13] Quantification of S1PR2 levels would greatly contribute to studies of examining sex differences in MS, and the identification of patients that may benefit from treatment using S1PR2 antagonists, which are less likely to cause lymphopenia.[14] Combined with a suitable radiotracer, positron emission tomography (PET), a reliable well established noninvasive imaging method, is able to offer a unique sensitive way to quantitatively assess neurotransmitter receptors, enzymes, and transporters *in vivo*.[15] Currently PET is widely used in clinical diagnosis. Identifying a suitable PET tracer that can specifically assess the expression of S1PR2 *in vivo*, will ultimately lead to better understanding of the function of S1PR2 in the neuropathogenesis of MS.

The inbred SJL mouse strain has been used as a model of the sexual dimorphism observed in MS, as SJL females are more susceptible to experimental autoimmune encephalomyelitis (EAE) than males; and exhibit a relapsing-remitting disease pattern similar to that observed in MS patients.[16,17] Moreover, sex difference has also been found in the CNS expression of S1PR2 in SJL mice, especially in the cerebellum,[13] which provides a good target for the validation of new-synthesized S1PR2 radioligands.

Herein we report the design and synthesis of a series of S1PR2 ligands containing similar core structures to the well-known S1PR2 selective antagonist **JTE-013**.[18] *In vitro* competitive cell membrane binding assays are conducted to determine the binding affinities of the newly synthesized analogues towards S1PR1, S1PR2, and S1PR3. Radiosynthesis of a S1PR2 radioligand [^{11}C]**5a**, *in vivo* evaluation of [^{11}C]**5a** *via* autoradiography, biodistribution, and microPET studies on SJL mice are accomplished. Our studies suggest that [^{11}C]**5a** demonstrates sexual dimorphism of S1PR2 expression in the cerebellum of SJL mice.

2. Results

2.1. Chemistry

The synthesis of S1PR2 ligands starts with the construction of key hydrazine intermediate **3**. Condensation of 5-amino-1,3-dimethylpyrazole with ethyl isobutyrylacetate using acetic acid as the solvent afforded compound **1**.[19] The reaction yield was low when propionic acid was employed as the solvent. Moreover, it's very challenging to remove the acylated side product from the reaction of 5-amino-1,3-dimethylpyrazole with solvent propionic acid due to its close polarity as the product. However, use of acetic acid as the solvent allowed the separation of the product from the acylated side product. Bromination of **1** afforded compound **2**, followed by reaction with hydrazine to produce the key intermediate **3**. The 2-chloropyridine moiety was synthesized from commercially available 2-chloro-6-methoxyisonicotinic acid. Treatment of 2-chloro-6-methoxyisonicotinic acid with diphenylphosphoryl azide afforded acyl azide **4**. Reflux of compound **4** in toluene *in situ* produced the isocyanate. A solution of hydrazine **3** in tetrahydrofuran (THF) was subsequently added to the above solution to give the first target compound **5a** in moderate yield (Scheme 1).

Next, we focused on the modification of the methoxy group in compound **5a** to explore new analogues targeting on S1PR2. The syntheses of the target compounds **5b–5f** are depicted in Scheme 2. Reaction of methyl 2-chloroisonicotinate with silver(II) fluoride, followed a reported procedure[20] to introduce a fluorine atom on the pyridine ring to generate compound **6**. Saponification of compound **6** gave carboxylic acid **7** in quantitative yield. Conversion of the acid to azide provided acyl azide **8**, which was further reacted with hydrazine **3** to give target compound **5b**. By replacing one of the chlorine atoms in 2,6-dichloroisonicotinic acid with methoxyethoxy functional group generated intermediate **9**, which was readily converted to target compound **5c** using a similar procedure for preparing compound **5a**. Alternatively, hydrolysis of 2,6-dichloroisonicotinic acid with aqueous sodium hydroxide solution at 130 °C, followed by precipitation of the product by acidification using 6 M HCl, produced the compound **11** in high yield. Protection of **11** with chloromethyl methyl ether afforded two regioisomers **12** and **13** in a 5/1 ratio, which were readily separated. The esters were saponified to afford acids **14** and **16** in high yields. Both compounds were converted to the acyl azide and reacted with hydrazine **3** to provide target compounds **5d** and **5e**. Attempts to remove the methoxymethoxyl (MOM) protecting group in compound **5e** using hydrogen chloride/dioxane led to a complex resulted from the poor solubility of compound **5e** in the solvent. To resolve the difficulty, deprotection of the MOM group of **5e** was accomplished by using trifluoroacetic acid in dichloromethane that smoothly produced the C-11 radiolabeling precursor **18** in moderate yield. One of the chlorine atoms in 2,6-dichloroisonicotinic acid was converted into a fluoroethoxy group to afford fluorine containing intermediate **19**. Following the above mentioned procedure, compound **19** reacted with compound **3** to give the target compound **5f**.

2.2. *In vitro* competitive binding assay

The *in vitro* competitive binding assays against [^{32}P]-S1P for the new synthesized target compounds **5a–5f** were conducted following our published protocol.[21] Results showed that com-

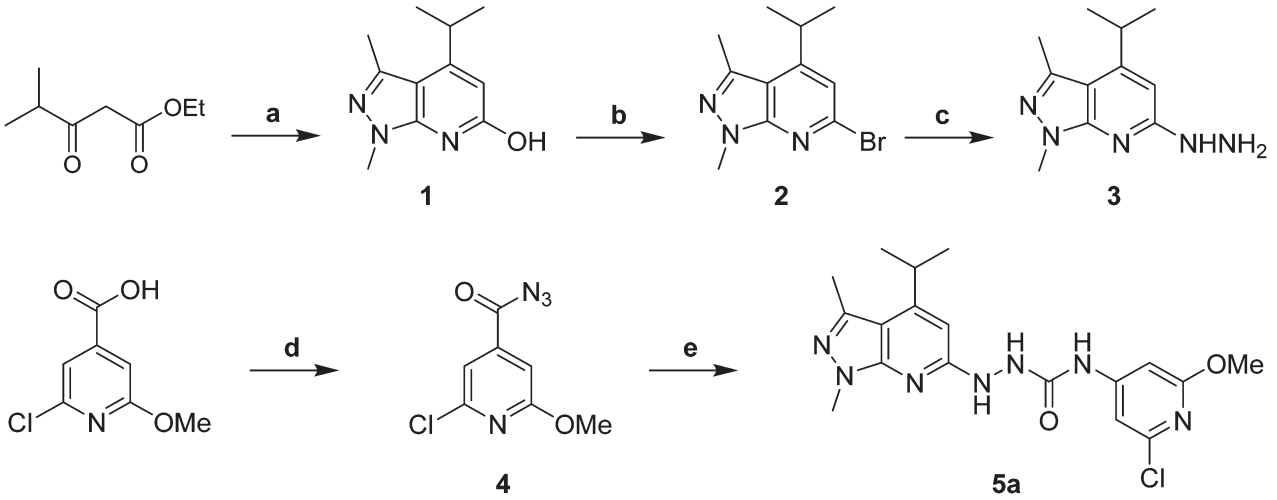

Scheme 1 Synthesis of the target compound **5a**. Reagents and conditions: (a) 5-amino-1,3-dimethylpyrazole, acetic acid, 140 °C, overnight, 18%; (b) $POBr_3$, anisole, reflux, 54%; (c) NH_2NH_2, EtOH, reflux, 92%; (d) diphenylphosphoryl azide, Et_3N, EtOAc, 57%; (e) (i) toluene, reflux; (ii) THF, **3**, 50 °C, 32% over two steps.

pounds **5a**, **5e**, and **5f** exhibited promising binding potency with IC_{50} value of 9.52 ± 0.70 nM, 8.09 ± 0.91 nM, 8.12 ± 0.62 nM, respectively, while compounds **5b** (IC_{50} = 135 ± 21 nM) and **5c** (IC_{50} = 234 ± 34 nM) only had moderate binding potency towards S1P2 receptor. No binding potency was observed for compound **5d** towards S1PR2. More importantly, compound **5a** was seven-fold more potent than the well-known S1PR2 antagonist – **JTE-013** (IC_{50} = 68.47 ± 7.45 nM, Fig. 1) and also showed good selectivity towards S1P1 and S1P3 receptors (IC_{50} > 1000 nM) (Table 1). Compounds **5a**, **5e**, **5f** showed similar calculated Log $D_{7.4}$ values as **JTE-013** except the calculated Log $D_{7.4}$ for compound **5d** was 1.01, which may cause it to lose binding potency for S1PR2.

2.3. Radiochemistry

With the promising *in vitro* competitive binding potency for several ligands having IC_{50} < 10 nM, we elected to radiolabel **5a** using [^{11}C]methyl iodide to make [^{11}C]**5a** for further *in vivo* validation. Various labeling conditions in terms of ^{11}C-methylating agents, reaction temperature, base, mobile phase were explored, the optimized reaction conditions of this reaction were: 1.0–1.3 mg precursor, 200 μL DMF, 3 μL of 5 M aqueous KOH solution, 85 °C, 5 min (Scheme 3). Under optimized semi-preparative HPLC conditions (Agilent Zorbax SB-C18 column, 250 × 9.2 mm, mobile phase 45% acetonitrile in 0.1 M ammonium formate, pH 6.5, flow rate 4.0 mL min^{-1}, detection wavelength 254 nm), the retention time was 15–17 min for [^{11}C]**5a**, 4–5 min for precursor **18**, and 5–6 min for a radioactive vice-product. It took about 40 min starting from the release of [^{11}C]methyl iodide to formation of the final injection dose of [^{11}C]**5a** with radiochemistry yield of 20 ± 5% (decayed to the end of bombardment (EOB), n > 10), specific activity of 222–370 GBq μmol^{-1} (EOB).

2.4. Biodistribution study

Biodistribution studies were conducted to assess the tracer uptake in the brain and peripheral organs/tissues. The uptake of [^{11}C]**5a** in female SJL mice at 30 min post injection showed that the heart, lung, kidney and liver had the highest uptake, which was consistent with S1PR2 distribution in mice.[22] The cerebellum and total brain displayed moderate tracer accumulation with the ID% per gram values of 0.84 ± 0.04 and 0.78 ± 0.04 respectively. Pretreatment of mice with Cyclosporin A (CsA), which improves blood brain barrier permeability *via* modulation of P-glycoprotein (P-gp) with inhibition of the ATP binding cassette efflux transporters,[23,24] the cerebellar uptake (ID% per g) within female mice was notably increased to 2.21 ± 0.21 (n = 4, p < 0.01) upon CsA treatment. The uptake of [^{11}C]**5a** in lung, thymus, kidney and liver showed similar trend in the CsA treatment group shown in Table 2.

2.5. *Ex vivo* autoradiography and microPET/computerized tomography (CT) study

To further validate the application of [^{11}C]**5a** for imaging S1PR2, *ex vivo* autoradiography studies and microPET/CT scans in male and female SJL mice with CsA pre-treatment were also performed. The results from both autoradiography and PET/CT studies consistently demonstrated higher accumulation of [^{11}C]**5a** in the cerebellum of female SJL mice than that observed in males (indicated by white dashed circles in Fig. 2A). Furthermore, quantitative microPET analysis showed that the average cerebellar uptake of [^{11}C]**5a** in female mice was statistically higher (n = 5, p = 0.021) than that in male mice (standardized uptake values (SUV) 0.58 ± 0.16 *vs.* 0.48 ± 0.12, Fig. 2B). The autoradiography and microPET/CT scans clearly demonstrated a sex difference in the cerebellar tracer uptake of [^{11}C]**5a** in SJL mice and was consistent with our pre-

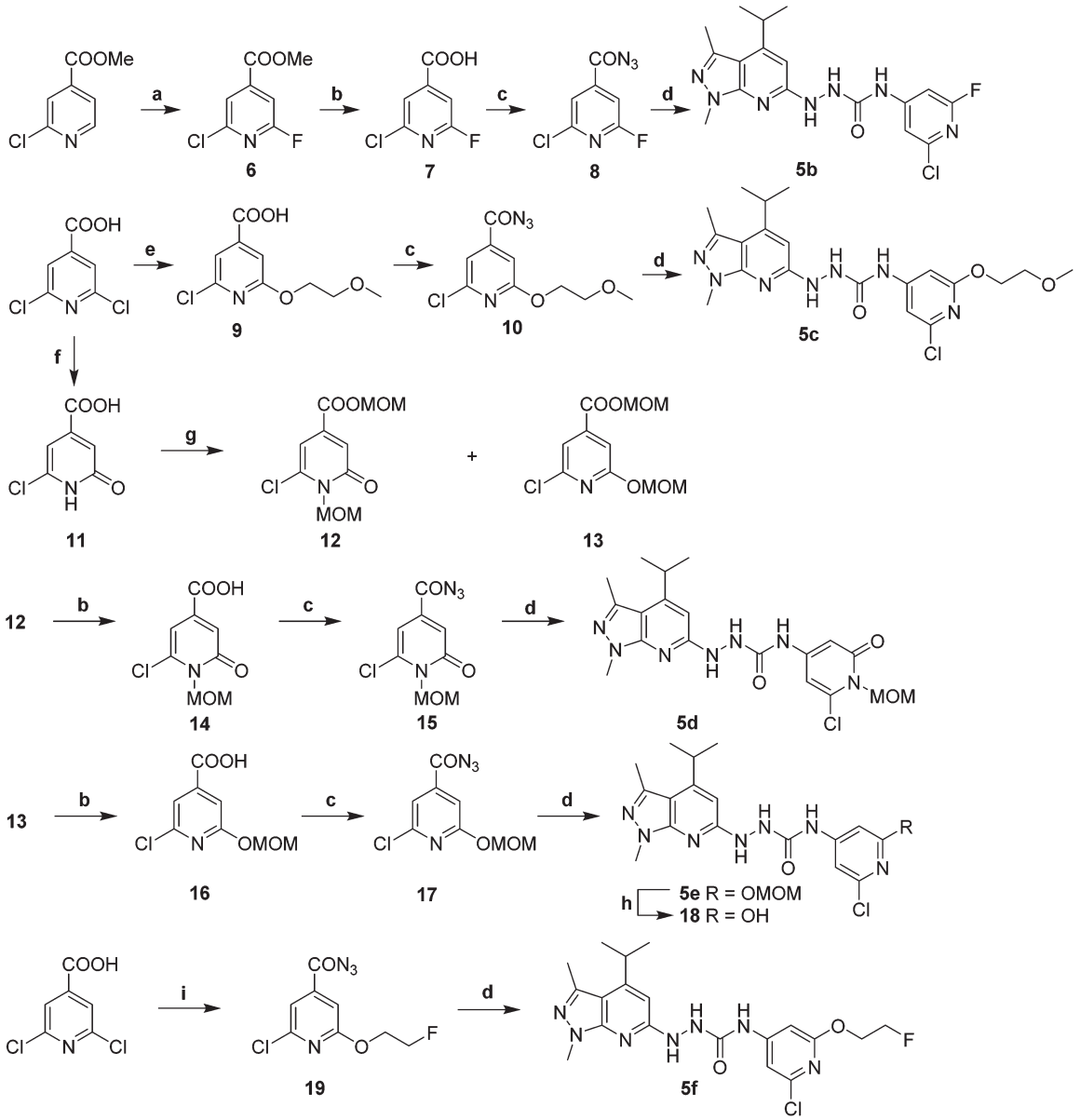

Scheme 2 Synthesis of target compounds **5b–5f**. Reagents and conditions: (a) silver(II) fluoride, acetonitrile; (b) LiOH, THF/H_2O (1/2, v/v), then 1 M HCl; (c) diphenylphosphoryl azide, Et_3N, 1,4-dioxane; (d) (i) toluene, reflux; (ii) THF, hydrazine **3**, 50 °C; (e) 2-methoxyethanol, ^tBuOK, THF; (f) (i) 2 M aqueous NaOH, 130 °C; (ii) 6 M HCl; (g) MOMCl, DIPEA, CH_2Cl_2; (h) TFA, CH_2Cl_2, 0 °C to rt, 2 h; (i) (i) 2-fluoroethanol, ^tBuOK, THF; (ii) diphenylphosphoryl azide, Et_3N, 1,4-dioxane.

vious report of S1PR2 expression in the cerebellum of SJL mice,[13] which support the target selectivity and specificity of this newly developed S1PR2 radiotracer.

3. Discussion

Our previous study revealed that S1PR2 plays an essential role in regulating blood–brain barrier (BBB) function during demyelinating CNS disease.[13] Development of a reliable and noninvasive imaging method that detects S1PR2 expression levels will facilitate better understanding of the neuropathologenesis of MS, especially with regard to the role of S1PR2 in neuroinflammation. Here we reported the design and synthesis of six S1PR2 ligands containing similar core structures as the well-known S1PR2 selective antagonist **JTE-013.** The synthesis took 6–9 steps. The synthesized ligands **5a–5f** were tested for binding potency towards S1PR1, S1PR2, and S1PR3 by *in vitro* competitive cell membrane binding assay. Three compounds showed good binding potency (IC_{50} < 10 nM) for S1PR2, and high selectivity over S1PR1 and S1PR3. Based on the *in vitro* data, we conclude that minor optimization of the

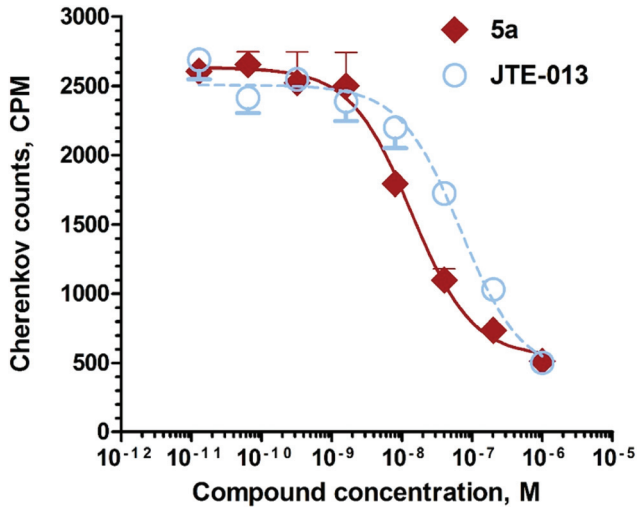

Fig. 1 Competitive binding curves of compound **5a** and **JTE-013** for S1PR2. A CHO cell membrane containing recombinant human S1PR2 was used in a [^{32}P]S1P competitive binding assay to measure the binding affinity for compound **5a** (red line, fitted IC_{50} = 9.52 ± 0.70 nM) and **JTE-013** (blue dashed line, fitted IC_{50} = 68.47 ± 7.45 nM).

functional group may led to significant change on the binding affinities, which will be useful for our future exploring the these structures reported in this manuscript.

The radiolabeling for the [^{11}C]**5a** was challenging due to two competitive *O*-^{11}C-methylation and *N*-^{11}C-methylation product formulated in the reaction. To increase the desired *O*-^{11}C-methylation radiolabeling product, different conditions in terms of reaction temperature, ^{11}C-methylating agents including [^{11}C]methyl iodide and [^{11}C]methyl triflate, base and mobile phase were tested (see Table S1†). Although cesium carbonate was reported to be an optimized base for the *O*-^{11}C-methylation of similar pyridin-2-ol substrates,[25,26] only moderate yield was achieved in our reaction when using cesium carbonate as the base. In our system, we observed that potassium hydroxide combined with [^{11}C]methyl iodide gave the highest *O*-^{11}C-methylation to *N*-^{11}C-methylation ratio compared to other conditions including [^{11}C]MeOTf/KOH, [^{11}C]MeI/Cs_2CO_3, [^{11}C]MeI/CsOH. Using pH 6.5 buffered aqueous ammonium formate solution improved resolution and radiochemical purity over pH 4.5 buffered aqueous ammonium formate. Under the optimized semi-preparative HPLC conditions, [^{11}C]**5a** with retention time at 15–17 min was separated well from the precursor **18** (t_R = 4–5 min) and radiolabeled by-product (t_R = 5–6 min). [^{11}C]**5a** was synthesized in about 40 min starting from the release of [^{11}C]methyl iodide to formation of the final injection dose with radiochemistry yield of 20 ± 5% (decayed to EOB, n > 10), specific activity of 222–370 GBq μmol^{-1} (EOB).

Biodistribution study of [^{11}C]**5a** indicated a higher cerebellar uptake of the tracer in female SJL mice with CsA pre-treat-

Table 1 Binding affinities (IC_{50} values, nM) of new synthesized compounds towards S1P2, S1P2, S1P3 receptors

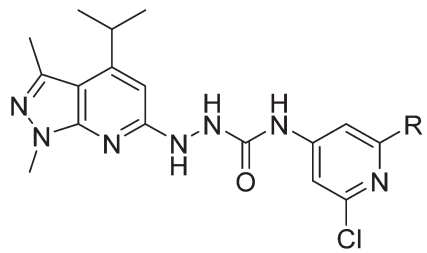

JTE-013 R = Cl
5a R = OMe
5b R = F
5c R = OCH_2CH_2OMe
5e R = OCH_2OMe
5f R = OCH_2CH_2F

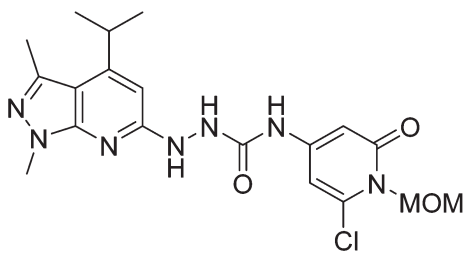

5d

Compound	c Log $D_{7.4}$ [a]	IC_{50} (nM) S1PR2	S1PR1	S1PR3
JTE-013	4.37	68.47 ± 7.45	>1000	>1000
5a	4.43	9.52 ± 0.70	>1000	>1000
5b	3.36	135 ± 21	>1000	>1000
5c	4.10	234 ± 34	>1000	>1000
5d	1.01	>1000	>1000	>1000
5e	3.83	8.09 ± 0.91	>1000	>1000
5f	4.66	8.12 ± 0.62	>1000	>1000

[a] Calculated value at pH = 7.4 by ACD/I-Lab ver. 7.0 (Advanced Chemistry Development, Inc., Canada).

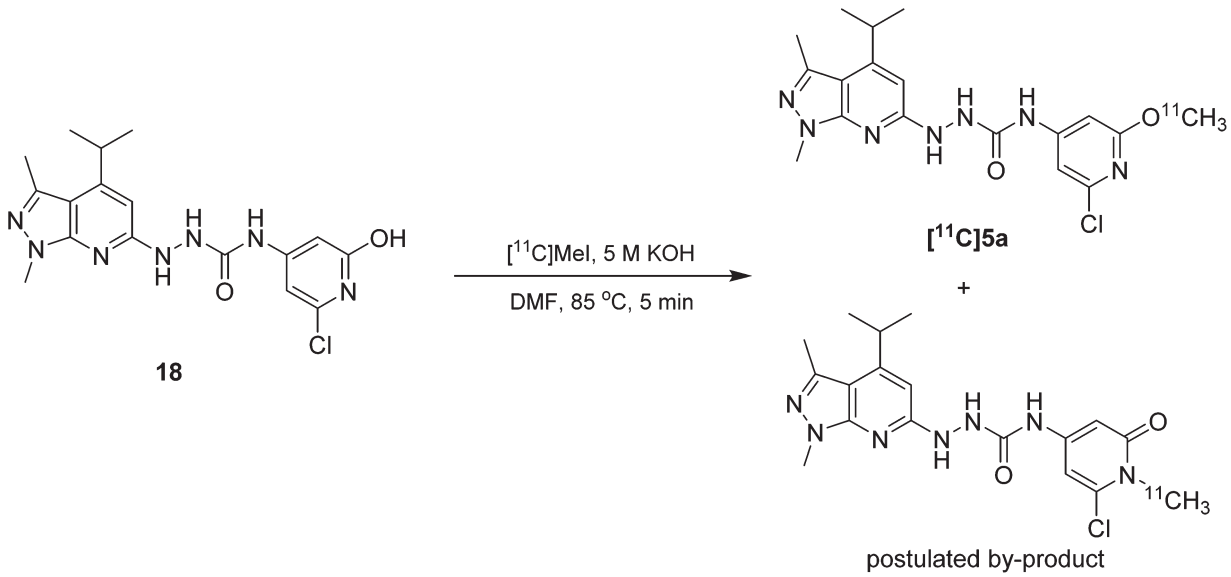

Scheme 3 Radiolabeling of the precursor **18** for [^{11}C]**5a** and postulated by-product.

Table 2 Biodistribution of [^{11}C]**5a** at 30 min post-injection in control *versus* CsA pre-treated female SJL mice

ID% per g	Female control	Female with CsA
Blood	3.52 ± 0.29	5.55 ± 0.61
Heart	3.56 ± 0.56	5.89 ± 0.62
Lung	5.71 ± 0.47	13.79 ± 2.56
Muscle	1.81 ± 0.18	2.65 ± 0.30
Fat	3.30 ± 0.54	3.13 ± 1.70
Thymus	2.81 ± 0.16	4.60 ± 0.22
Spleen	2.95 ± 0.24	3.99 ± 0.39
Kidney	7.96 ± 1.29	9.43 ± 0.96
Liver	13.31 ± 1.34	15.91 ± 1.06
Cerebellum	0.84 ± 0.04	2.21 ± 0.21
Total brain	0.78 ± 0.04	1.96 ± 0.18

ment than that in control the group. It is notable that CsA increased the cerebellar uptake of [^{11}C]**5a** in female SJL mice by ~2.6-fold, which suggest the brain uptake towards [^{11}C]**5a** is modestly modulated by P-gp[27–29] and thus is limited. Although species difference is common in P-gp transport of radioligands[30] and [^{11}C]**5a** may have relatively high uptake in monkey or human brains. On the other hand, the low brain uptake of [^{11}C]**5a** might also be partially attributed to the relatively low S1PR2 expression level in the brain, since the localization of S1PR2 in SJL mice brain is mainly on endothelial cells.[13] Structural optimization of **5a** in the pyrazole-pyridine moiety to avoid P-gp efflux transport and enhance BBB penetration, while retaining binding potency is ongoing. Among the synthesized ligands, compound **5e** with a fluoroethoxy group also displayed high binding potency (IC_{50} = 8.09 ± 0.91 nM). Here

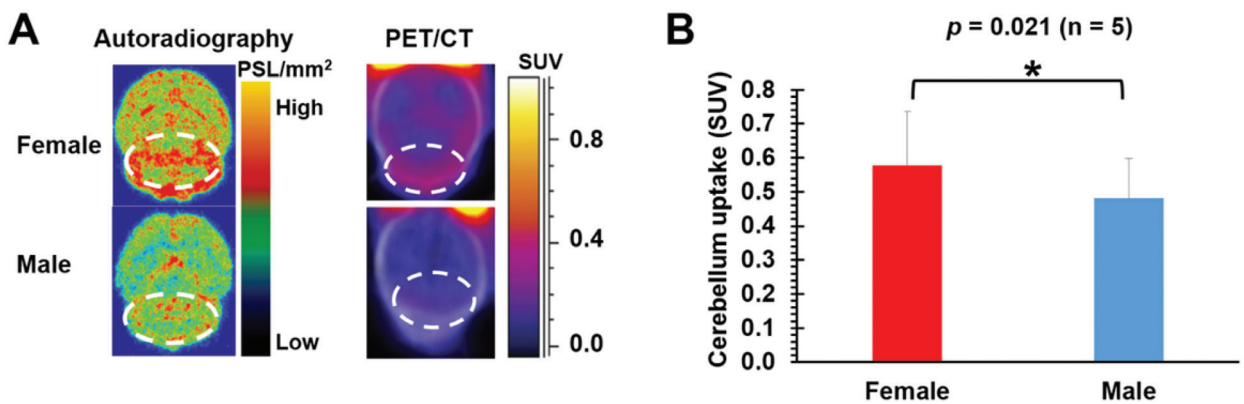

Fig. 2 (A) Autoradiography and PET/CT images of [^{11}C]**5a** in the brains of female and male SJL mice (n = 5) upon CsA pre-treatment; (B) quantification of cerebellar uptake of [^{11}C]**5a** in female and male SJL mice upon CsA treatment from microPET. All the histograms were average values from 5 independent experiments, error bars were the standard derivations.

we focused on our first investigation of [^{11}C]**5a** as a S1PR2 PET ligand. Exploration of **5f** and other F-18 labeled ligands is undergoing within our group.

While the pathogenesis of MS involves both genetic susceptibility in terms of immune function and activation,[31] and environmental causes such as Epstein-Barr virus infections,[32] studies focused on sex differences are needed for new insights into hormonal and genetic sex-related factors that may impact on disease susceptibility and to identify new treatment targets. In addition, defined biomarkers that improve diagnostic evaluation and treatment follow-up in a sex-specific fashion are urgently needed. The identification of sex differences in S1PR2 expression and signaling in the neuropathogenesis of CNS autoimmunity[13] is a critical step towards gender-based medicine for the treatment of MS. Targeting S1PR2 may also treat MS without impacting normal immune function. Detection of S1PR2 *via* a novel, sensitive and noninvasive imaging PET modality will improve the assessment of the receptor *in vivo.* The current developed tracer meets the above requirement and is able to detect the sexual dimorphism of S1PR2 expression within autoimmune susceptible SJL mice in terms of biodistribution, autoradiography, microPET/CT scans.

4. Conclusions

We designed and synthesized a spectrum of S1PR2 ligands, chose a ligand that has high binding potency and high selectivity for S1P receptor 2 to be labeled with [^{11}C]methyl iodide. Utilizing the radioligand [^{11}C]**5a**, we successively demonstrated the sexual dimorphism of S1PR2 expression in SJL mice with CsA pre-treatment. Further exploring the lead structures to identify a promising radioligands for S1PR2 with ability to penetrate the blood brain barrier, may greatly contribute to the diagnosis and treatment of MS and other neuroinflammatory diseases.

5. Materials and methods

5.1. Chemistry

General. All reagents and chemicals were purchased from commercial suppliers and used without further purification unless otherwise stated. Melting points were determined on a MEL-TEMP 3.0 apparatus and are uncorrected. ^{1}H NMR and ^{13}C NMR spectra were recorded at 300 or 400 MHz on a Varian Mercury-VX spectrometer using $CDCl_3$, Acetone-d6, CD_3OD, DMSO-d6 as solvent. All chemical shift values were reported in parts per million (ppm) (δ). The following abbreviations were used to describe peak patterns wherever appropriate: br = broad, s = singlet, d = doublet, t = triplet, q = quartet, m = multiplet. HRMS analyses were conducted in Washington University Resource for Biomedical and Bio-organic Mass Spectrometry. Preparative chromatography was performed on Chemglass chromatography column using 230–400 mesh silica gel purchase from Silicycle. Analytical TLC was carried out on Merck 60 F_{254} silica gel glass plates, and visualization was aided by UV.

4-Isopropyl-1,3-dimethyl-1*H*-pyrazolo[3,4-*b*]pyridin-6-ol (1).[33] A mixture of 5-amino-1,3-dimethylpyrazole (5.4 g, 49 mmol) and ethyl isobutyrylacetate (10 g, 63 mmol) in acetic acid (100 mL) was heated at 140 °C in a sealed tube for 20 h, the mixture was concentrated to remove the solvent and subjected to silica gel chromatography using CH_2Cl_2/MeOH (20/1) as the eluent to afford compound **1** (1.8 g, 18% yield) as a light yellow solid. ^{1}H NMR (400 MHz, $CDCl_3$) δ 6.14 (s, 1H), 3.96 (s, 3H), 3.32–3.22 (m, 1H), 2.49 (s, 3H), 1.27 (d, J = 6.4 Hz, 6H).

6-Bromo-4-isopropyl-1,3-dimethyl-1*H*-pyrazolo[3,4-*b*]pyridine (2).[33] To a solution of **1** (1.0 g, 4.9 mmol) in anisole (10 mL) was added phosphorus oxybromide (2.0 g, 7.0 mmol). The reaction was heated at 130 °C overnight. Water was added to quench the reaction which was then extracted with EtOAc. The combined organic layers were washed with saturated aqueous $NaHCO_3$, and saturated aqueous NaCl. The organic phase was concentrated *in vacuo*, and the residue was subjected to silica gel chromatography using CH_2Cl_2/MeOH (30/1) as the eluent to afford compound **2** (0.70 g, 54% yield) as a light yellow solid. ^{1}H NMR (400 MHz, $CDCl_3$) δ 6.99 (s, 1H), 3.95 (s, 3H), 3.53–3.43 (m, 1H), 2.59 (s, 3H), 1.28 (d, J = 6.8 Hz, 6H).

6-Hydrazinyl-4-isopropyl-1,3-dimethyl-1*H*-pyrazolo[3,4-*b*]pyridine (3).[33] To a solution of **2** (0.45 g, 1.7 mmol) in ethanol (1.0 mL) was added anhydrous hydrazine (2.8 g, 88 mmol). The reaction was heated in a sealed tube at 120 °C overnight. The mixture was concentrated *in vacuo*, and the residue was subjected to silica gel chromatography using CH_2Cl_2/MeOH (20/1) as the eluent to afford compound **3** (0.34 g, 92% yield) as a yellow solid. ^{1}H NMR (400 MHz, $CDCl_3$) δ 6.14 (s, 1H), 4.00 (br, 2H), 3.84 (s, 3H), 3.40–3.30 (m, 1H), 2.50 (s, 3H), 1.21 (d, J = 7.2 Hz, 6H).

2-Chloro-6-methoxyisonicotinoyl azide (4). To a solution of 2-chloro-6-methoxyisonicotinic acid (0.28 g, 1.5 mmol) in ethyl acetate (3 mL) was added Et_3N (0.38 g, 3.8 mmol). The solution was cooled to 0 °C and diphenylphosphoryl azide (0.45 g, 1.7 mmol) was added dropwise. The reaction was warmed to room temperature upon addition and was stirred overnight. The mixture was concentrated *in vacuo*, and the residue was subjected to silica gel chromatography using hexane/EtOAc (30/1) as the eluent to afford compound **4** (0.18 g, 57% yield) as a white solid. Mp 67–69 °C; ^{1}H NMR (400 MHz, Acetone-d6) δ = 7.21 (s, 1H), 6.99 (s, 1H), 3.82 (s, 3H); ^{13}C NMR (100.7 MHz, Acetone-d6) δ 169.8, 164.5, 149.3, 142.9, 114.5, 108.9, 54.2; HRMS (ESI) calcd for $C_7H_6ClN_4O_2$ 213.0179, $[M + H]^+$, found 213.0174.

***N*-(2-Chloro-6-methoxypyridin-4-yl)-2-(4-isopropyl-1,3-dimethyl-1*H*-pyrazolo[3,4-*b*]pyridin-6-yl)hydrazine-1-carboxamide (5a).** Under nitrogen, a solution of **4** (40 mg, 0.19 mmol) in toluene (0.5 mL) was refluxed for 3 hours to *in situ* produce the isocyanate. The reaction mixture was allowed to cool to 50 °C and a solution of **3** (31 mg, 0.14 mmol) in anhydrous THF (1 mL) was added dropwise. The reaction was then stirred at 50 °C overnight. The mixture was concentrated *in vacuo*, and the residue was subjected to silica gel chromatography using

CH_2Cl_2/MeOH (20/1) as the eluent to afford compound **5a** (18 mg, 32% yield) as a light yellow solid. Mp 243–245 °C; ^{1}H NMR (400 MHz, CD_3OD) δ 7.09 (s, 1H), 6.82 (s, 1H), 6.40 (s, 1H), 3.74 (s, 3H), 3.73 (s, 3H), 3.42–3.37 (m, 1H), 2.45 (s, 3H), 1.22 (d, J = 6.4 Hz, 6H); ^{13}C NMR (100.7 MHz, CD_3OD) δ 166.6, 164.7, 160.0, 156.2, 150.6, 148.5, 145.9, 140.0, 110.0, 106.2, 99.1, 96.1, 53.1, 31.8, 29.4, 21.7, 13.4; HRMS (ESI) calcd for $C_{18}H_{22}ClN_7NaO_2$ 426.1421, $[M + Na]^+$, found 426.1403.

Methyl 2-chloro-6-fluoroisonicotinate (6). To a solution of methyl 2-chloroisonicotinate (1.0 g, 6.0 mmol) in anhydrous acetonitrile (50 mL) was added silver(II) fluoride (2.6 g, 18 mmol) under nitrogen. The reaction was stirred in a sealed tube at 40 °C overnight. The suspension was filtered through Celite and the solution was concentrated by rotary evaporation. The residue was subjected to silica gel chromatography using hexane/EtOAc (40/1) as the eluent to afford compound **6** (0.25 g, 0.58 g of the starting material was recovered, 50% yield based on recovered starting material) as a clear liquid. This compound is a known compound and commercially available. ^{1}H NMR (400 MHz, Acetone-d6) δ 7.65–7.63 (m, 1H), 7.37–7.36 (m, 1H), 3.85 (s, 3H).

2-Chloro-6-fluoroisonicotinic acid (7). To a solution of **6** (0.24 g, 1.3 mmol) in THF (2 mL) was added aqueous lithium hydroxide solution (40 mg in 4 mL water, 1.6 mmol) dropwise at 0 °C. The reaction was stirred at room temperature overnight. 2 M $HCl_{(aq)}$ was added to neutralize the reaction. The mixture was extracted with EtOAc, the combined organic layers were dried over sodium sulfate. The concentrated residue was subjected to silica gel chromatography using CH_2Cl_2/MeOH (3/1) as the eluent to afford compound **7** (0.22 g, 99% yield) as a white soild. Mp 118–120 °C; ^{1}H NMR (400 MHz, CD_3OD) δ 7.52 (s, 1H), 7.20 (d, J = 1.6 Hz, 1H); ^{13}C NMR (100.7 MHz, CD_3OD) δ 164.7, 162.7 (d, J = 245.3 Hz), 148.8 (d, J = 14.2 Hz), 148.2, 121.3 (d, J = 12.2 Hz), 107.8 (d, J = 44.2 Hz); HRMS (ESI) calcd for $C_6H_4ClFNO_2$ 175.9915, $[M + H]^+$, found 175.9905.

2-Chloro-6-fluoroisonicotinoyl azide (8). To a solution of **7** (0.10 g, 0.57 mmol) in anhydrous 1,4-dioxane (2 mL) was added Et_3N (0.12 g, 1.1 mmol). The solution was cooled to 0 °C and diphenylphosphoryl azide (0.31 g, 1.1 mmol) was added dropwise. The reaction was warmed to room temperature upon addition and was stirred overnight. The mixture was concentrated *in vacuo*, and the residue was subjected to silica gel chromatography using hexane/EtOAc (50/1) as the eluent to afford compound **8** (35 mg, 31% yield) as a yellow solid. Mp 39–40 °C; ^{1}H NMR (400 MHz, Acetone-d6) δ 7.71 (s, 1H), 7.44 (d, J = 2.0 Hz, 1H); ^{13}C NMR (100.7 MHz, Acetone-d6) δ 169.0, 162.8 (d, J = 244.9 Hz), 149.3, 145.8, 120.9, 107.8 (d, J = 43.6 Hz).

***N*-(2-Chloro-6-fluoropyridin-4-yl)-2-(4-isopropyl-1,3-dimethyl-1*H*-pyrazolo[3,4-*b*]pyridin-6-yl)hydrazine-1-carboxamide (5b).** Under nitrogen, a solution of **8** (30 mg, 0.15 mmol) in toluene (0.8 mL) was refluxed for 3 hours to *in situ* produce the isocyanate. The reaction mixture was allowed to cool to 50 °C and a solution of **3** (30 mg, 0.12 mmol) in anhydrous THF (0.8 mL) was added dropwise. The reaction was then stirred at 50 °C overnight. The mixture was concentrated *in vacuo*, and the residue was subjected to silica gel chromatography using CH_2Cl_2/MeOH (30/1) as the eluent to afford compound **5b** (8 mg, 17% yield) as a light yellow solid. Mp 166–168 °C; ^{1}H NMR (400 MHz, $CDCl_3$) δ 8.16 (br, 1H), 7.26 (s, 1H), 7.14 (s, 1H), 6.61 (br, 1H), 6.44 (br, 1H), 6.40 (s, 1H), 3.85 (s, 3H), 3.50–3.43 (m, 1H), 2.55 (s, 3H), 1.26 (d, J = 6.8 Hz, 6H); ^{13}C NMR (100.7 MHz, $CDCl_3$) δ 164.4, 163.0, 156.3 (d, J = 225.1 Hz), 150.8, 150.6, 149.2, 140.2, 110.5, 110.3, 97.5, 96.8, 96.4, 33.3, 29.8, 22.9, 15.3; HRMS (ESI) calcd for $C_{17}H_{19}ClFN_7NaO$ 414.1221, $[M + Na]^+$, found 414.1207.

2-Chloro-6-(2-methoxyethoxy)isonicotinic acid (9). To a solution of 2,6-dichloroisonicotinic acid (1.1 g, 5.7 mmol) in anhydrous THF (5 mL) was added a solution of potassium *tert*-butoxide (1.6 g, 14.3 mmol) in THF (14 mL) dropwise at 0 °C. 30 min later, 2-methoxyethanol was added dropwise and the reaction was continued at room temperature overnight. 1 N aqueous hydrochloric acid was added to adjust the solution pH to 4. The mixture was extracted with EtOAc, the combined organic layers were dried over sodium sulfate. The concentrated residue was subjected to silica gel chromatography using CH_2Cl_2/MeOH (4/1) as the eluent to afford compound **9** as a white solid (1.6 g, 98% yield). Mp 138–140 °C; ^{1}H NMR (400 MHz, CD_3OD) δ 7.36 (s, 1H), 7.17 (s, 1H), 4.41 (t, J = 5.2 Hz, 2H), 3.71 (t, J = 4.4 Hz, 2H), 3.38 (s, 3H); ^{13}C NMR (100.7 MHz, CD_3OD) δ 164.9, 163.8, 148.7, 143.8, 115.5, 109.4, 70.3, 65.8, 57.7; HRMS (ESI) calcd for $C_9H_{11}ClNO_4$ 232.0377, $[M + H]^+$, found 232.0368.

2-Chloro-6-(2-methoxyethoxy)isonicotinoyl azide (10). To a solution of **9** (0.15 g, 0.65 mmol) in anhydrous 1,4-dioxane (2 mL) was added Et_3N (0.10 g, 0.97 mmol). The solution was cooled to 0 °C and diphenylphosphoryl azide (0.27 g, 0.97 mmol) was added dropwise. The reaction was warmed to room temperature upon completion of the addition and was stirred overnight. The mixture was concentrated *in vacuo*, and the residue was subjected to silica gel chromatography using hexane/EtOAc (20/1) as the eluent to afford compound **10** (200 mg, 84% yield) as a light yellow liquid. ^{1}H NMR (400 MHz, Acetone-d6) δ 7.25 (s, 1H), 7.05 (s, 1H), 4.33 (t, J = 4.4 Hz, 2H), 3.58 (t, J = 4.8 Hz, 2H), 3.22 (s, 3H); ^{13}C NMR (100.7 MHz, Acetone-d6) δ 169.9, 164.2, 149.1, 143.2, 114.6, 109.1, 70.1, 66.5, 57.9; HRMS (ESI) calcd for $C_9H_{10}ClN_4O_3$ 257.0441, $[M + H]^+$, found 257.0436.

***N*-(2-Chloro-6-(2-methoxyethoxy)pyridin-4-yl)-2-(4-isopropyl-1,3-dimethyl-1*H*-pyrazolo[3,4-*b*]pyridin-6-yl)hydrazine-1-carboxamide (5c).** A solution of **10** (126 mg, 0.49 mmol) in toluene (1.2 mL) was refluxed at 120 °C for 3 hours under nitrogen to *in situ* produce the isocyanate. To the above mixture was added dropwise a solution of **3** (140 mg, 0.64 mmol) in anhydrous THF (1.2 mL) at 50 °C. The reaction continued to stir at 50 °C for overnight. The mixture was concentrated *in vacuo*, and the residue was subjected to silica gel chromatography using CH_2Cl_2/MeOH (30/1) as the eluent to afford compound **5c** (78 mg, 35% yield) as a light yellow solid. Mp 210–212 °C; ^{1}H NMR (400 MHz, $CDCl_3$) δ 8.22 (br, 1H), 7.45 (br, 1H), 7.07 (br, 1H), 6.99 (s, 1H), 6.84 (s, 1H), 6.36 (s, 1H), 4.36 (t, J = 4.0 Hz, 2H), 3.80 (s, 3H), 3.65 (t, J = 4.4 Hz, 2H), 3.41–3.38 (m, 1H), 3.35 (s, 3H), 2.50 (s, 3H), 1.21 (d, J = 6.8 Hz, 6H); ^{13}C NMR

(100.7 MHz, $CDCl_3$) δ 163.8, 158.4, 156.7, 156.2, 150.5, 149.1, 148.7, 140.0, 109.6, 106.9, 97.7, 97.3, 70.8, 65.6, 58.9, 33.2, 29.6, 22.8, 15.1; HRMS (ESI) calcd for $C_{20}H_{26}ClN_7NaO_3$ 470.1683, $[M + Na]^+$, found 470.1674.

6-Chloro-2-oxo-1,2-dihydropyridine-4-carboxylic acid (11). 2,6-Dichloroisonicotinic acid (2.5 g, 13 mmol) was added to 2 N aqueous NaOH solution (32 mL). The solution was refluxed at 130 °C for overnight. 6 N HCl was added to the solution to precipitate the product when the solution was cooled down to room temperature. The suspension was filtered and the white solid was collected, dried *in vacuo* to afford the product **11** (2.2 g, 99% yield) as a white solid. Mp 186–188 °C; ^{1}H NMR (400 MHz, DMSO-d6) δ 12.82 (br, 1H), 7.18 (s, 1H), 7.02 (s, 1H); ^{13}C NMR (100.7 MHz, DMSO-d6) δ 165.2, 164.8, 148.3, 144.7, 114.3, 108.9; HRMS (ESI) calcd for $C_6H_5ClNO_3$ 173.9958, $[M + H]^+$, found 173.9946.

Methoxymethyl 6-chloro-1-(methoxymethyl)-2-oxo-1,2-dihydropyridine-4-carboxylate (12)/methoxymethyl 2-chloro-6-(methoxymethoxy)isonicotinate (13). To a solution of compound **11** (0.87 g, 5 mmol) in CH_2Cl_2 (100 mL) was added i-Pr_2NEt (3.2 g, 25 mmol). The solution was cooled to 0 °C and chloromethyl methyl ether (1.6 g, 20 mmol) was added dropwise. The reaction was warmed to room temperature after completion of the addition and stirred overnight. The solution was quenched with water and extracted with CH_2Cl_2. The combined organic phase was washed with saturated aqueous $NaHCO_3$, saturated sodium chloride solution, and dried with anhydrous sodium sulfate. The concentrated residue was subjected to silica gel chromatography using CH_2Cl_2/MeOH (40/1) as the eluent to afford compound **12** (polar, 876 mg, 67% yield) as a clear liquid and **13** (less polar, 180 mg, 14% yield) as a clear liquid.

Compound **12**: ^{1}H NMR (400 MHz, $CDCl_3$) δ 7.11 (s, 1H), 6.73 (s, 1H), 5.56 (s, 2H), 5.39 (s, 2H), 3.48 (s, 3H), 3.39 (s, 3H); ^{13}C NMR (100.7 MHz, $CDCl_3$) δ 163.12, 163.05, 140.4, 138.4, 121.3, 105.5, 92.1, 75.8, 58.1, 57.8; HRMS (ESI) calcd for $C_{10}H_{12}ClNNaO_5$ 284.0302, $[M + Na]^+$, found 284.0300.

Compound **13**: ^{1}H NMR (400 MHz, $CDCl_3$) δ 7.40 (d, J = 0.8 Hz, 1H), 7.20 (d, J = 0.8 Hz, 1H), 5.43 (s, 2H), 5.40 (s, 2H), 3.47 (s, 3H), 3.44 (s, 3H); ^{13}C NMR (100.7 MHz, $CDCl_3$) δ 163.1, 162.8, 149.2, 142.5, 116.7, 109.8, 92.8, 91.9, 58.0, 57.3; HRMS (ESI) calcd for $C_{10}H_{12}ClNNaO_5$ 284.0302, $[M + Na]^+$, found 284.0289.

6-Chloro-1-(methoxymethyl)-2-oxo-1,2-dihydropyridine-4-carboxylic acid (14). To a solution of **12** (1.4 g, 5.3 mmol) in THF (5 mL) was added an aqueous solution of lithium hydroxide (0.17 g in 10 mL water, 7.0 mmol) dropwise at 0 °C. The reaction was stirred at room temperature for overnight. 2 N HCl solution was added to acidify the reaction. The mixture was extracted with EtOAc, the combined organic phase was dried over sodium sulfate. The concentrated residue was subjected to silica gel chromatography using CH_2Cl_2/MeOH (4/1) as the eluent to afford compound **14** (0.82 g, 71% yield) as a white solid. Mp 161–163 °C; ^{1}H NMR (400 MHz, CD_3OD) δ 6.94 (s, 1H), 6.74 (s, 1H), 5.52 (s, 2H), 3.30 (s, 3H); ^{13}C NMR (100.7 MHz, CD_3OD) δ 164.5, 163.9, 142.3, 138.3, 119.7, 106.2, 75.7, 56.4; HRMS (ESI) calcd for $C_8H_8ClNNaO_4$ 240.0040, $[M + Na]^+$, found 240.0034.

6-Chloro-1-(methoxymethyl)-2-oxo-1,2-dihydropyridine-4-carbonyl azide (15). To a solution of **14** (0.41 g, 1.9 mmol) in anhydrous 1,4-dioxane (16 mL) was added Et_3N (0.28 g, 2.8 mmol). The solution was cooled to 0 °C and diphenylphosphoryl azide (0.77 g, 2.8 mmol) was added dropwise. The reaction was warmed to room temperature upon completion of the addition and stirred overnight. The mixture was concentrated *in vacuo*, and the residue was subjected to silica gel chromatography using hexane/EtOAc (6/1) as the eluent to afford compound **15** (0.28 g, 62% yield) as a yellow solid. Mp 99–100 °C; ^{1}H NMR (400 MHz, $CDCl_3$) δ 7.06 (s, 1H), 6.69 (s, 1H), 5.55 (s, 2H), 3.39 (s, 3H); ^{13}C NMR (100.7 MHz, Acetone-d6) δ 170.0, 162.1, 140.7, 138.9, 120.4, 103.5, 75.6, 56.7; HRMS (ESI) calcd for $C_{16}H_{15}Cl_2N_8O_6$ 485.0492, $[2M + H]^+$, found 485.0490.

***N*-(6-Chloro-1-(methoxymethyl)-2-oxo-1,2-dihydropyridin-4-yl)-2-(4-isopropyl-1,3-dimethyl-1*H*-pyrazolo[3,4-*b*]pyridin-6-yl)hydrazine-1-carboxamide (5d).** A solution of **15** (75 mg, 0.31 mmol) in toluene (2 mL) was refluxed for 3 hours under nitrogen to *in situ* produce the isocyanate. To the above mixture was added dropwise a solution of **3** (53 mg, 0.24 mmol) in anhydrous THF (2 mL) at 60 °C. The reaction continued to stir at 60 °C overnight. The mixture was concentrated *in vacuo*, and the residue was subjected to silica gel chromatography using CH_2Cl_2/MeOH (40/1) as the eluent to afford compound **5d** (92 mg, 88% yield) as a light yellow solid. Mp 172–174 °C; ^{1}H NMR (400 MHz, CD_3OD) δ 6.77 (s, 1H), 6.71 (s, 1H), 6.43 (s, 1H), 5.43 (s, 2H), 3.79 (s, 3H), 3.45–3.38 (m, 1H), 3.32 (s, 3H), 2.49 (s, 3H), 1.25 (d, J = 6.8 Hz, 6H); ^{13}C NMR (100.7 MHz, CD_3OD) δ 164.6, 159.7, 155.6, 150.8, 150.0, 139.8, 137.6, 107.9, 102.1, 100.2, 98.6, 98.5, 74.9, 56.2, 31.9, 29.4, 21.9, 13.7; HRMS (ESI) calcd for $C_{19}H_{24}ClN_7NaO_3$ 456.1527, $[M + Na]^+$, found 456.1514.

2-Chloro-6-(methoxymethoxy)isonicotinic acid (16). To a solution of **13** (0.48 g, 1.8 mmol) in THF (2.4 mL) was added aqueous lithium hydroxide solution (57 mg in 4.8 mL water, 2.4 mmol) dropwise at 0 °C. The reaction was stirred at room temperature overnight. 2 N $HCl_{(aq)}$ was added to neutralize the reaction at 0 °C. The mixture was extracted with EtOAc, the combined organic phase was dried over sodium sulfate. The concentrated residue was subjected to silica gel chromatography using CH_2Cl_2/MeOH (4/1) as the eluent to afford compound **16** (0.31 g, 77% yield) as a light yellow solid. Mp 150–152 °C; ^{1}H NMR (400 MHz, Acetone-d6) δ 7.33 (s, 1H), 7.12 (s, 1H), 5.36 (s, 2H), 3.35 (s, 3H); ^{13}C NMR (100.7 MHz, acetone-d6) δ 164.0, 163.0, 148.7, 144.1, 116.6, 109.8, 92.7, 56.4; HRMS (ESI) calcd for $C_8H_8ClNNaO_4$ 240.0040, $[M + Na]^+$, found 240.0036.

2-Chloro-6-(methoxymethoxy)isonicotinoyl azide (17). To a solution of **16** (0.24 g, 1.1 mmol) in anhydrous 1,4-dioxane (5 mL) was added Et_3N (0.14 g, 1.4 mmol). The solution was cooled to 0 °C and diphenylphosphoryl azide (0.39 g, 1.4 mmol) was added dropwise. The reaction was warmed to room temperature and stirred overnight. The mixture was concentrated *in vacuo*, and the residue was subjected to silica gel

chromatography using hexane/EtOAc (50/1) as the eluent to afford compound **17** (0.11 g, 41% yield) as a yellow liquid. ^{1}H NMR (400 MHz, Acetone-d6) δ 7.35 (s, 1H), 7.14 (s, 1H), 5.41 (s, 2H), 3.38 (s, 3H); ^{13}C NMR (100.7 MHz, Acetone-d6) δ 181.1, 169.8, 163.2, 149.0, 115.7, 109.2, 92.9, 56.4; the acyl azide was converted to free amine during mass analysis. HRMS (ESI) calcd for $C_7H_9ClN_2NaO_2$ 211.0250, $[M + Na]^+$, found 211.0243.

***N*-(2-Chloro-6-(methoxymethoxy)pyridin-4-yl)-2-(4-isopropyl-1,3-dimethyl-1*H*-pyrazolo[3,4-*b*]pyridin-6-yl)hydrazine-1-carboxamide (5e).** A solution of **17** (108 mg, 0.45 mmol) in toluene (2.2 mL) was refluxed at 120 °C for 3 hours under nitrogen to *in situ* produce the isocyanate. To the above mixture was added dropwise a solution of **3** (76 mg, 0.35 mmol) in anhydrous THF (2.5 mL) at 50 °C. The reaction continued to stir at 50 °C for overnight. The mixture was concentrated *in vacuo*, and the residue was subjected to silica gel chromatography using CH_2Cl_2/MeOH (40/1) as the eluent to afford compound **5e** (130 mg, 86% yield) as a pale white solid. Mp 208–209 °C; ^{1}H NMR (400 MHz, CD_3OD) δ 7.25 (s, 1H), 7.00 (s, 1H), 6.48 (br, 1H), 5.37 (s, 2H), 3.81 (s, 3H), 3.53–3.46 (m, 1H), 3.44 (s, 3H), 2.54 (s, 3H), 1.31 (d, J = 6.8 Hz, 6H); ^{13}C NMR (100.7 MHz, CD_3OD) δ 163.0, 159.9, 155.7, 151.1, 150.9, 148.5, 139.9, 107.8, 107.0, 98.6, 98.5, 96.9, 92.0, 55.8, 31.7, 29.3, 21.8, 13.6; HRMS (ESI) calcd for $C_{19}H_{24}ClN_7NaO_3$ 456.1527, $[M + Na]^+$, found 456.1515.

***N*-(2-Chloro-6-hydroxypyridin-4-yl)-2-(4-isopropyl-1,3-dimethyl-1*H*-pyrazolo[3,4-*b*]pyridin-6-yl)hydrazine-1-carboxamide (18).** Compound **5e** (54 mg, 0.12 mmol) was dissolved in CH_2Cl_2 (2 mL). Trifluoroacetic acid (1 mL) was added dropwise at 0 °C. The solution was stirred at room temperature for 2 hours. Saturated aqueous $NaHCO_3$ solution was added to quench the reaction. The mixture was extracted with CH_2Cl_2. The combined organic phase was dried over sodium sulfate and concentrated through rotary evaporation. The residue was subjected to silica gel chromatography using CH_2Cl_2/MeOH (10/1) as the eluent to afford the precursor **18** (21 mg, 43% yield) for radiolabeling. Mp 226–228 °C; ^{1}H NMR (400 MHz, CD_3OD) δ 6.90 (s, 1H), 6.71 (s, 1H), 6.40 (s, 1H), 3.74 (s, 3H), 3.46–3.37 (m, 1H), 2.46 (s, 3H), 1.24 (d, J = 6.8 Hz, 6H); ^{13}C NMR (100.7 MHz, CD_3OD) δ 164.7, 159.9, 158.0, 155.7, 151.4, 151.0, 140.8, 139.9, 107.8, 103.3, 98.6, 98.5, 31.7, 29.4, 21.8, 13.6; HRMS (ESI) calcd for $C_{17}H_{21}ClN_7O_2$ 390.1445, $[M + H]^+$, found 390.1441.

2-Chloro-6-(2-fluoroethoxy)isonicotinoyl azide (19). To a solution of 2,6-dichloroisonicotinic acid (0.96 g, 5 mmol) in anhydrous THF (5 mL) was added a solution of potassium *tert*-butoxide (1.4 g, 12.5 mmol) in THF (12 mL) dropwise at 0 °C. 5 min later, 2-fluoroethanol (480 mg, 7.5 mmol) was added dropwise and the reaction was continued at room temperature for overnight. 1 N aqueous hydrochloric acid was added to adjust the solution pH to 4.0. The mixture was extracted with EtOAc, the combined organic phase was dried with sodium sulfate, and concentrated *in vacuo* to give the crude ether. The ether was then dissolved in anhydrous 1,4-dioxane (10 mL). Et_3N (0.18 mL, 1.3 mmol), diphenylphosphoryl azide (0.36 g, 1.3 mmol) was added successively. The reaction was stirred at room temperature overnight. The mixture was concentrated *in vacuo*, and the residue was subjected to silica gel chromatography using hexane/EtOAc (20/1) as the eluent to afford compound **19** (103 mg, 8% yield for two steps) as a yellow solid. Mp 47–48 °C; ^{1}H NMR (400 MHz, Acetone-d6) δ 7.26 (s, 1H), 7.07 (s, 1H), 4.66 (dt, J = 47.6 Hz, 4.0 Hz, 2H), 4.47 (dt, J = 29.2 Hz, 4.0 Hz, 2H); ^{13}C NMR (100.7 MHz, Acetone-d6) δ 169.8, 163.8, 149.0, 143.4, 115.1, 109.2, 81.4 (d, J = 209.1 Hz), 66.5 (d, J = 24.3 Hz).

***N*-(2-Chloro-6-(2-fluoroethoxy)pyridin-4-yl)-2-(4-isopropyl-1,3-dimethyl-1*H*-pyrazolo[3,4-*b*]pyridin-6-yl)hydrazine-1-carboxamide (5f).** A solution of **19** (64 mg, 0.26 mmol) in toluene (1.5 mL) was refluxed for 3 hours under nitrogen to *in situ* produce the isocyanate. To the above mixture was added dropwise a solution of **3** (44 mg, 0.2 mmol) in anhydrous THF (2 mL) at 50 °C. The reaction continued to stir at 50 °C for overnight. The mixture was concentrated *in vacuo*, and the residue was subjected to silica gel chromatography using CH_2Cl_2/MeOH as the eluent to afford compound **5f** (54 mg, 62% yield) as a pale solid. Mp 240–242 °C; ^{1}H NMR (400 MHz, CD_3OD) δ 7.20 (s, 1H), 6.93 (s, 1H), 6.47 (s, 1H), 4.64 (dt, J = 47.6 Hz, 3.6 Hz, 2H), 4.42 (dt, J = 25.2 Hz, 4.0 Hz, 2H), 3.81 (s, 3H), 3.52–3.42 (m, 1H), 2.52 (s, 3H), 1.30 (d, J = 6.8 Hz, 6H); ^{13}C NMR (100.7 MHz, CD_3OD) δ 163.7, 159.9, 155.7, 150.9, 150.8, 148.3, 139.9, 119.7, 106.7, 98.6, 98.5, 96.5, 81.4 (d, J = 209.1 Hz), 65.5 (d, J = 24.3 Hz), 31.7, 29.4, 21.8, 13.6; HRMS (ESI) calcd for $C_{19}H_{23}ClFN_7NaO_2$ 458.1483, $[M + Na]^+$, found 458.1492.

5.2. Radiochemistry

Production of $[^{11}C]CH_3I$ followed the reported method.[34] Briefly, $[^{11}C]CH_3I$ was produced on-site using a GE PETtrace MeI Microlab through consecutive reaction starting from $[^{11}C]CO_2$. Up to 1400 mCi of $[^{11}C]CO_2$ was produced from the JSW BC-16/8 cyclotron by irradiating a gas target of 0.5% O_2 in N_2 for 15–30 min with a 40 μA beam of 16 MeV protons in the Barnard Cyclotron Facility of Washington University School of Medicine. $[^{11}C]CH_3I$ was produced by reduction of $[^{11}C]CO_2$ using a nickel catalyst (Shimalite-Ni (reduced), Shimadzu, Japan P.N.221-27719) in the presence of hydrogen gas at 360 °C, followed by iodination of the resulting $[^{11}C]CH_4$ with iodine at 690 °C. Approximately 12.2 min following the end-of-bombardment (EOB), 800–1000 mCi of $[^{11}C]CH_3I$ were delivered *via* gas tubing to the reaction vial in the hot cell.

$[^{11}C]CH_3I$ was bubbled for a period of 2–3 min into a solution of precursor (1.0–1.3 mg) in DMF (0.2 mL) containing 3.0 μL of potassium hydroxide (5.0 M) at room temperature. When the trap of radioactivity was completed, the sealed reaction vessel was heated at 85 °C for 5 min, shaking was applied to the vial using a long clamp during the reaction. The oil bath was removed and 1.7 mL of the HPLC mobile phase (45% acetonitrile in 0.1 M ammonium formate, v/v, pH 6.5) was added into to the reaction vessel. The mixture was loaded onto a reversed phase HPLC system to purify the mixture (Agilent Zorbax SB-C18 column, 250 × 9.2 mm, mobile phase 45% acetonitrile in 0.1 M ammonium formate, pH 6.5, flow rate 4.0 mL min^{-1}, detection wavelength 254 nm). Under these conditions, the product with retention time at 15–17 min was col-

lected into a vial that contained 50 mL Milli-Q water. Then the collected fraction was passed through a C-18 Plus Sep-Pak® cartridge to concentrate the target component in the Sep-Pak cartridge. The Sep-Pak cartridge was rinsed using 20 mL of sterile water. Finally, the tracer trapped on the Sep-Pak® was eluted with 0.3 mL of ethanol, following with 2.7 mL 0.9% sodium chloride solution, passing through a 0.22 μm (Whatman Puradisc 13 mm syringe filter) sterile filter into a sterile pyrogen-free glass vial for delivery. For quality control, an aliquot of sample was assayed by an analytical HPLC system (Agilent Zorbax SB-C18 column, 250 × 4.6 mm, mobile phase 55% acetonitrile in 0.1 M ammonium formate, pH 4.5, flow rate 1.2 mL min^{-1}, detection wavelength 254 nm). The sample was authenticated by co-injecting with the corresponding nonradiolabeled standard solution. The retention time was 5.5 min with radiochemical purity was >99%. The radiosynthesis typically took 40 min starting from the release of [^{11}C]methyl iodide, with yield 20 ± 5% (n > 10, decay corrected to the end of synthesis), specific activity 222–370 GBq μmol^{-1} (decayed to EOB).

5.3. *In vitro* competitive binding assay

In vitro competitive binding assay against [^{32}P]S1P assay was conducted according to our published protocol.[21]

5.4. Biodistribution, autoradiography, PET/CT study

All animal experiments were conducted in compliance with the Guidelines for the Care and Use of Research Animals under protocols approved by Washington University's Animal Studies Committee. For mice biodistribution studies, 64–89 μCi of [^{11}C]**5a** was injected *via* the tail vein (i.v.) into mature female SJL mice (n = 4 per study group, mice weight 18–24 g) under 2–3% isoflurane/oxygen anesthesia. Eight mice were divided into two groups: the control group without CsA pre-treatment and the CsA pre-treatment group (25 mg kg^{-1} of CsA, i.v. 30 min prior to the tracer injection). At 30 min post-injection (p.i.), mice were anesthetized again and euthanized. The whole brain was quickly harvested, the blood was removed by blotting, and the cerebellum was separated, the remainder of the brain was collected to determine the total brain uptake. Peripheral organs and tissues, including blood, heart, lung, muscle, fat, thymus, spleen, kidney, and liver, were also collected; all samples were weighed and counted in an automated well counter with a standard dilution of the injectate. Counts were decay-corrected and the %ID per g was calculated. A two-tailed paired Student's t test was used to calculate the standard derivations. A p value less than 0.05 was considered statistically significant.

For the *ex vivo* autoradiography study, SJL mice were injected with 400–900 μCi of [^{11}C]**5a** and euthanized 30 min p.i. as described above. The whole brain was quickly removed and snap-frozen. Horizontal sections (100 μm) were cut with a Microm cryotome and mounted on Superfrost Plus glass slides (Fisher Scientific, Pittsburgh, PA). Frozen slides were directly exposed to film in an imaging cassette for 4 hours at −80 °C in the dark. The distribution of radioactivity was visualized by a Fuji Bio-Imaging Analyzer FLA-7000 (Fuji Photo Film Co., Tokyo, Japan). Photo-stimulated luminescence (PSL) from the cerebellum was quantified using Multi Gauge v3.0 software (Fuji Photo Film Co., Tokyo, Japan). Data were background-corrected and expressed as photo-stimulated luminescence signals per square millimeter (PSL per mm^2).

Brain microPET imaging was performed using two Siemens microPET scanners (Siemens Preclincial Solutions, Knoxville, TN, USA) – microPET-Focus-F220 and a microPET-Inveon Multi-Modality scanners. Imaging studies were done using 19–25 g SJL mice pretreated with Cyclosporin A. Animals were anesthetized using 2% isoflurane/oxygen and a tail vein catheter placed in the lateral tail vein. Gas anesthesia was maintained at <1.5% isoflurane during the imaging session; each mice was positioned on the scanner bed at least 30 min prior to the tracer injection. Body temperature was maintained using a warming lamp. A dose of 25 mg kg^{-1} CsA in saline administered i.v. 30 min prior to radiotracer injection was used for modulation of the BBB efflux transporters. Both CsA and the radiotracer (400–900 μCi of [^{11}C]**5a**) were administered using an i.v. catheter placed in the lateral tail vein. The imaging sessions were carried out as 1 h dynamic scan using the MicroPET Focus 220 and Inveon scanners (Siemens Medical Solutions USA). Acquired list mode data were histogrammed into a 3D set of sinograms and binned to the following time frames: 1 × 3 s, 6 × 2 s, 9 × 5 s, 6 × 10 s, 4 × 30 s, 2 × 60 s, 2 × 2 min, 10 × 5 min. Sinogram data was then processed using filter back projection algorithm with attenuation and scatter corrections. Regions of interest (the cerebellum) were manually drawn with the software ASIPro (Acquisition Sinogram Image Processing, Siemens Medical Solutions, Malvern, PA, USA) using IDL's Virtual Machine (ITT Visual Information Solutions, Boulder, CO, USA) to calculate the average cerebellar uptake.

Acknowledgements

This work was financially supported by the USA DOE-Training Grant: #DESC0008432 and the Washington University, Mallinckrodt Institute of Radiology (MIR) Pilot Grant: #14-017, the USA National Institute of Mental Health (NIMH) of the National Institutes of Health (no. MH092797) and National Institute of Neurological Disorders and Stroke (NINDS, no. NS075527, NS061025, P01 NS059560), and National Multiple Sclerosis Society grants PP2043, RG 4632.

References

1 D. H. Mahad, B. D. Trapp and H. Lassmann, *The Lancet. Neurology*, 2015, **14**, 183–193.
2 R. M. Ransohoff, D. A. Hafler and C. F. Lucchinetti, *Nat. Rev. Neurol.*, 2015, **11**, 134–142.
3 *McAlpine's Multiple Sclerosis. Section 1: The story of multiple sclerosis*, Elsevier, Churchill, Livingstone, Philadelphia, 2006.
4 A. Compston and A. Coles, *Lancet*, 2008, **372**, 1502–1517.

5 A. E. Handel, L. Jarvis, R. McLaughlin, A. Fries, G. C. Ebers and S. V. Ramagopalan, *PLoS One*, 2011, **6**, e14606.
6 S. M. Orton, B. M. Herrera, I. M. Yee, W. Valdar, S. V. Ramagopalan, A. D. Sadovnick and G. C. Ebers, *The Lancet. Neurology*, 2006, **5**, 932–936.
7 B. G. Weinshenker, B. Bass, G. P. Rice, J. Noseworthy, W. Carriere, J. Baskerville and G. C. Ebers, *Brain: J. Neurol.*, 1989, **112**(Pt 6), 1419–1428.
8 H. Tremlett, Z. Yinshan and V. Devonshire, *Mult. Scler.*, 2008, **14**, 314–324.
9 D. Marsolais and H. Rosen, *Nat. Rev. Drug Discovery*, 2009, **8**, 297–307.
10 L. Kappos, E. W. Radue, P. O'Connor, C. Polman, R. Hohlfeld, P. Calabresi, K. Selmaj, C. Agoropoulou, M. Leyk, L. Zhang-Auberson and P. Burtin, *N. Engl. J. Med.*, 2010, **362**, 387–401.
11 D. Pelletier and D. A. Hafler, *N. Engl. J. Med.*, 2012, **366**, 339–347.
12 E. Roberts, M. Guerrero, M. Urbano and H. Rosen, *Expert Opin. Ther. Pat.*, 2013, **23**, 817–841.
13 L. Cruz-Orengo, B. P. Daniels, D. Dorsey, S. A. Basak, J. G. Grajales-Reyes, E. E. McCandless, L. Piccio, R. E. Schmidt, A. H. Cross, S. D. Crosby and R. S. Klein, *J. Clin. Invest.*, 2014, **124**, 2571–2584.
14 G. T. Kunkel, M. Maceyka, S. Milstien and S. Spiegel, *Nat. Rev. Drug Discovery*, 2013, **12**, 688–702.
15 M. Inglese and M. Petracca, *Prion*, 2013, **7**, 47–54.
16 T. L. Papenfuss, C. J. Rogers, I. Gienapp, M. Yurrita, M. McClain, N. Damico, J. Valo, F. Song and C. C. Whitacre, *J. Neuroimmunol.*, 2004, **150**, 59–69.
17 T. M. Rivers, D. H. Sprunt and G. P. Berry, *J. Exp. Med.*, 1933, **58**, 39–53.
18 C. Li, X. X. Chi, W. Xie, J. A. Strong, J. M. Zhang and G. D. Nicol, *J. Neurophysiol.*, 2012, **108**, 1473–1483.
19 N. L. Nam, I. I. Grandberg and V. I. Sorokin, *Chem. Heterocycl. Compd.*, 2003, 937–942.
20 P. S. Fier and J. F. Hartwig, *Science*, 2013, **342**, 956–960.
21 A. J. Rosenberg, H. Liu and Z. Tu, *Appl. Radiat. Isot.*, 2015, **102**, 5–9.
22 M. Adada, D. Canals, Y. A. Hannun and L. M. Obeid, *FEBS J.*, 2013, **280**, 6354–6366.
23 Z. Tu, S. Li, J. Xu, W. Chu, L. A. Jones, R. R. Luedtke and R. H. Mach, *Nucl. Med. Biol.*, 2011, **38**, 725–739.
24 W. Loscher and H. Potschka, *NeuroRx: J. Am. Soc. Exp. Neurotherapeutics*, 2005, **2**, 86–98.
25 M. D. Moran, A. A. Wilson, C. S. Elmore, J. Parkes, A. Ng, O. Sadovski, A. Graff, Z. J. Daskalakis, S. Houle, M. J. Chapdelaine and N. Vasdev, *Bioorg. Med. Chem.*, 2012, **20**, 4482–4488.
26 C. N. Wang, C. K. Moseley, S. M. Carlin, C. M. Wilson, R. Neelamegam and J. M. Hooker, *Bioorg. Med. Chem. Lett.*, 2013, **23**, 3389–3392.
27 K. Ishiwata, K. Kawamura, K. Yanai and N. H. Hendrikse, *J. Nucl. Med.*, 2007, **48**, 81–87.
28 E. F. J. De Vries, J. Doorduin, N. A. R. Vellinga, A. Van Waarde, R. A. Dierckx and H. C. Klein, *Nucl. Med. Biol.*, 2008, **35**, 459–466.
29 K. A. Kurdziel, D. O. Kiesewetter, R. E. Carson, W. C. Eckelman and P. Herscovitch, *J. Nucl. Med.*, 2003, **44**, 1330–1339.
30 S. Syvanen, O. Lindhe, M. Palner, B. R. Kornum, O. Rahman, B. Langstrom, G. M. Knudsen and M. Hammarlund-Udenaes, *Drug Metab. Dispos.*, 2009, **37**, 635–643.
31 P. A. Gourraud, H. F. Harbo, S. L. Hauser and S. E. Baranzini, *Immunol. Rev.*, 2012, **248**, 87–103.
32 A. Ascherio and K. L. Munger, *Annals Neurol.*, 2007, **61**, 288–299.
33 R. E. Swenson, *PCT Int. Appl*, 2013 WO 2013148460 A1 20131003.
34 Z. Tu, C. S. Dence, D. E. Ponde, L. Jones, K. T. Wheeler, M. J. Welch and R. H. Mach, *Nucl. Med. Biol.*, 2005, **32**, 423–430.